Structure of a Parallel-Stranded Tetramer of the *Oxytricha* Telomeric DNA Sequence dT_4G_4†

Goutam Gupta,‡ Angel E. Garcia,‡ Qiu Guo,§,∥ Min Lu,§,⊥ and Neville R. Kallenbach*,§

Los Alamos National Laboratory, Group T-10, Mail Stop K710, Los Alamos, New Mexico 87545, and Department of Chemistry, New York University, New York, New York 10003

Received December 11, 1992; Revised Manuscript Received April 28, 1993

ABSTRACT: We report here the determination of the solution structure of the single-copy tetramer of the sequence dT_4G_4, the unit repeat in telomeres of the ciliated protozoan *Oxytricha*, in the presence of potassium ions. This is accomplished by a combination of sequential assignments and distance determinations from 2D proton NMR with model building, based on conformational analysis of the structure using a full-matrix NOESY simulation and molecular dynamics. Each strand in this tetramer structure has an identical environment and conformation: a parallel-stranded, right-handed helix, with all nucleotides in the C2′-*endo*, *anti* configuration. The T flanking the G cluster stacks in a 4-fold symmetrical helical array, while the remaining T's become increasingly flexible and sample multiple stacked configurations.

The ends of eukaryotic chromosomes are protected by telomeres, nucleoprotein structures that stabilize the ends against damage and provide a mechanism for complete replication of the genome without ablation of the 3′ termini [reviewed in Blackburn (1991)]. The DNA from telomeres contains repeated clusters of G residues on one strand, with complementary C clusters on the other; the G-rich strand terminates in two copies of the G cluster that form an overhang at the 3′ end (Klobutcher et al., 1981; Henderson & Blackburn, 1989). Duplex DNA molecules with copies of G clusters cohere to form higher molecular weight aggregates (Lipps, 1980; Oka & Thomas, 1987; Acevedo et al., 1991). This association is favored by potassium ions (Acevedo et al., 1991), as is the aggregation of guanosine or GMP monomers (Gellert et al., 1962). Model oligonucleotides containing telomeric sequences form different tetraplex-containing structures, depending on the number of copies present, the sequence and number of G's in the cluster, and the addition of monovalent ions such as sodium or potassium (Henderson et al., 1987; Sen & Gilbert, 1988, 1990; Williamson et al., 1990; Sundquist & Klug, 1989; Kang et al., 1992; Smith & Feigon, 1992). Single copies of the telomeric repeat have been shown to form a tetramer in the presence of sodium or potassium, with exceptional thermal stability in the presence of potassium (Lu et al., 1992).

Physical or chemical damage to the DNA at a chromosome end can, in principle, yield chains containing one, two, or more single-strand copies of the G cluster, the associative properties of which would act to prevent dissociation of the fragmented strands (Yu & Blackburn, 1991). Experiments on oligonucleotide models encoding one, two, or four copies of a telomeric G-rich sequence reveal a variety of putative tetraplex H-bonded structures involving the G bases (Henderson et al., 1987; Sen & Gilbert, 1988, 1990; Williamson et al., 1990; Sundquist & Klug, 1989; see Figure 1. A high-resolution crystal structure (Kang et al., 1992) and NMR solution data (Smith & Feigon, 1992) have recently been reported for the sequence $dG_4T_4G_4$ designed to provide a model for the two-copy 3′ G-rich strand terminal overhang. The most stable structure containing the *Oxytricha* sequence unit, dT_4G_4, is formed by association of four single-copy oligomers to form a tetramer in the presence of sodium or potassium (Figure 1a). The stoichiometry of this complex has been determined by the method of Hope and Struhl (1987), in which two oligomers with different chain lengths are mixed and annealed, and the resulting bands on native gel electrophoresis are counted (Sen & Gilbert, 1988, 1990; Lu et al.,

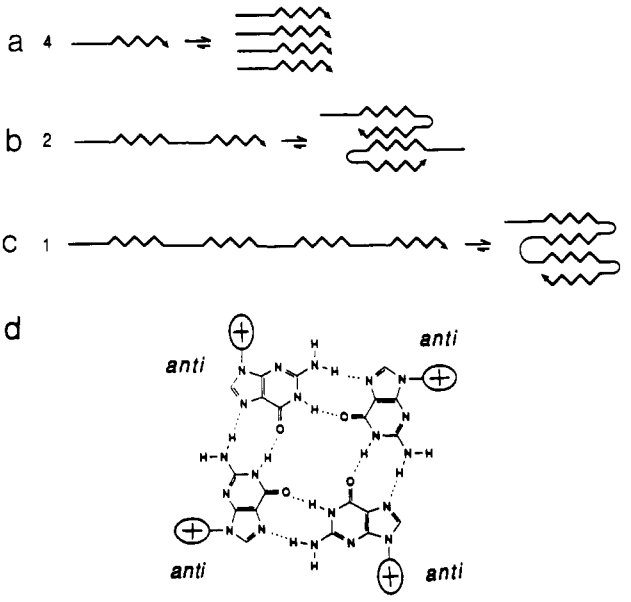

FIGURE 1: Proposed modes of interaction of the G clusters in dT_4G_4 oligomers with different numbers of repeats, in the presence of sodium or potassium: (a) parallel-stranded complex of four single-copy dT_4G_4 units (Sen & Gilbert, 1990; Lu et al., 1992a); (b) dimer of $G_4T_4G_4$ or $d(T_4G_4)_2$, with strands antiparallel (Sen & Gilbert, 1990; Kang et al., 1992; Lu et al., 1992a); (c) condensed structure formed by four-copy $d(T_4G_4)_4$ (Williamson et al., 1990); (d) the layer structure in a G-4 tetraplex, with G's forming cyclic Hoogsteen base pairs (Gellert et al., 1962; Arnott et al., 1974; Zimmerman et al., 1975).

† This research was supported by grants from the National Institutes of Health (CA 24101) and from the W. M. Keck Foundation (N.R.K.). Q.G. and M.L. are supported by NIH NRSA postdoctoral fellowships. This work is also supported by the U.S. Department of Energy.

* To whom correspondence should be addressed.

‡ Los Alamos National Laboratory.

§ New York University.

∥ Present address: Department of Biology, Massachusetts Institute of Technology, Cambridge, MA 02139.

⊥ Present address: Department of Biochemistry and Molecular Biology, Harvard University, Cambridge MA 02138.

0006-2960/93/0432-7098$04.00/0

1992). While ordered nucleic acids normally unfold on heating, in the presence of K^+, the tetramer structure in dT_4G_4 is remarkable in that it actually favors a more asymmetric structure at high temperature (Lu et al., 1992). The stability of this structure can best be understood in terms of its detailed conformation, namely, (1) the relative orientations of the four strands, (2) the H-bonding network involving G's and T's, (3) the stereochemistry of the G- and T-nucleotides and the handedness of the four strands, (4) the stacking interactions in the G- and T-tracts and at the T4-G5 step, and (5) the relative dynamics of the residues inside the G- and T-tracts and at the T4-G5 step. We have employed a combination of 1D/2D ^1H NMR and MD simulated annealing studies to derive these structural properties of the unit sequence dT_4G_4 from *Oxytricha* in the presence of K^+.

MATERIALS AND METHODS

DNA Synthesis. The DNA strands used in this study were synthesized on an ABI 391 DNA synthesizer and deprotected using routine phosphoramidite chemistry (Caruthers, 1983). The strands were purified by preparative HPLC on a Du Pont Zorbax Bio Series column, following the standard elution protocol. The sequence was confirmed by chemical methods (Lu et al., 1992).

NMR Experiments. 1D and 2D NMR spectral data were recorded on solutions of 2 mM dT_4G_4 in H_2O and D_2O in 10 mM phosphate buffer, 0.1 mM EDTA, and 200 mM KCl, pH 7.5. The 1D NMR spectra were recorded at temperatures from 25 to 80 °C. Determination of the structure of the complex was based on 2D NOESY/ROESY data on dT_4G_4 in D_2O recorded at 60 °C, to avoid higher associated states of the strands (Lu et al., 1992). 2D NMR data sets were obtained on a Varian Unity 500 spectrometer. Acquisition parameters for the NOESY (Wuthrich, 1986) and the rotating frame Overhauser effect (ROESY; Bax, 1988) experiments used were as follows: sweep width = 6500 Hz, complex data points in t_2 = 2048, complex FIDs in t_1 = 512, number of transients = 32, and relaxation delay = 1.5 s. The mixing times, τ_m, for NOESY and ROESY experiments were 100 and 60 ms, respectively. Spectra in water and 1D NOE data were acquired on a Bruker AM500 unit, using a 1331 pulse sequence for water suppression (Hore, 1983).

Sequential Assignments. The sequential assignment scheme used for the dT_4G_4 tetramer began with 1D NOEs connecting G NH protons to the H8 and NH_2 protons and 2D NOEs connecting the H8 protons of G to their own and adjacent H2′ and H2″ sugar protons, using cross sections from 2D NOESY and ROESY experiments carried out at various mixing times. Next the sugar spin systems involving H1′, H2′, H2″, H3′, and H4′ were sequentially assigned by monitoring the intranucleotide interactions between H1′–H2′, H1′–H2″, H2′–H3′, H2″–H3′, and H3′–H4′, again using both NOESY and ROESY experiments and cross sections from the 2D data sets in cases of spectral overlap. The methyl groups of T were sequentially assigned by means of internucleotide H6–CH_3 ROESY cross-peaks.

Structural Analysis. A general procedure developed for the analysis of structure and dynamics in conformationally mobile nucleic acids (Gupta et al., 1992) was applied to the 1D/2D NMR data on the dT_4G_4 tetramer. First, the H-bonding pattern in the tetramer was characterized by monitoring the temperature dependence and the solvent exchange properties of the imino signals in H_2O and by performing 1D NOE experiments. Second, a set of interproton distances (i.e., average values and associated dispersions) were extracted for various pairwise interactions by performing a full-matrix NOESY simulation (FMNS) with associated *R*-factor tests, comparing the calculated and the observed NOESY/ROESY intensities as described in Gupta et al. (1989). Third, these interproton distances were used as structural constraints in constant high-temperature (500 K) 100-ps MD simulations. A set of 100 "snapshots" (at 1-ps intervals) were extracted from the MD trajectory, and constrained energy minimization on each snapshot was used to map local minima on the sampled energy surface in the temperature quenching step (Stillinger & Weber, 1984). Finally, the FMNS procedure was repeated on each of the representative local minima to verify the agreement with the NOESY data.

Molecular dynamics and energy minimizations were performed using the all-atom force field of Weiner et al. (1986) in AMBER 3.0. All calculations were done *in vacuo* with a dielectric constant of 78.4 and without any nonbonding cutoff. The high-temperature (500 K) simulations were performed with a set of strong H-bonding constraints (k = 100 kcal mol^{-1} $Å^{-2}$) on the G·G pairs in the quartet. Strong constraints were also imposed on interproton distances ≤2.5 Å.

RESULTS

UV cross-linking of the T's in the dT_4G_4 tetramer is consistent with a parallel orientation of the strands, such that all four T sequences are spatially proximal (Lu et al., 1992). Investigation of this complex by ^1H NMR spectroscopy reveals conformational details of the backbone and pairing in the structure and makes it possible to investigate the dynamics of the molecule. The H-bonding network in the structure is characterized by performing 1D NOE experiments, while the conformational details of the nucleotides on each strand, including intra- and interstrand stacking interactions, the relative orientations of the four strands, and the handedness of the structure, emerge from 2D NOESY/ROESY experiments.

1D NMR Data on Exchangeable Protons: Structure of the G Core of the dT_4G_4 Tetramer. Figure 2a shows the slowly exchanging H-bonded NH protons of G at low field in a K^+ solution of dT_4G_4. Four imino protons resonate below 10 ppm; these are characteristic of H-bonded G·G pairs. The imino proton signals of G are unaffected on increasing the temperature from 25 to 75 °C, as shown in spectra 1–4; they remain in slow exchange beyond 80 °C. Even in 100% D_2O at 60 °C (spectrum 5), the two protons assigned to the internal bases in the G cluster (G6 and G7) are not fully exchanged. This behavior is consistent with formation of a tightly stacked and H-bonded G-quartet, as illustrated in Figure 1d and in the inset of Figure 2b. Observation of only four imino G protons indicates that the four strands forming the tetraplex (Lu et al., 1992) are structurally equivalent, in an identical environment. A G-tetraplex with four equivalent strands is anticipated to have four characteristic interproton distances that should lead to observable NOEs in the region of the ^1H spectrum seen in Figure 2b: (1) a direct NOE linking diagonal G imino protons from one layer to the next, NH(i)···NH(i+1), <3.6 Å; (2) an indirect intralayer NOE at H8 of G in the plane of the G-quartet, involving the NOE pathway NH···NH_2···H8, each step being <3.3 Å as shown in the inset; (3) longer range indirect interlayer NOEs between H8(i–1)···NH(i) (<5 Å) *via* the spin diffusion pathway, H8(i–1)···NH_2(i–1)···NH(i); and (4) interlayer NOEs linking H8(i+1) with NH(i) (>5.5 Å), principally *via* the diffusion pathway, NH(i)···NH(i+1)/NH_2(i+1)···H8(i+1). Observation of each of these connectivities allows sequential assignments of the NH and H8 resonances in the G core by

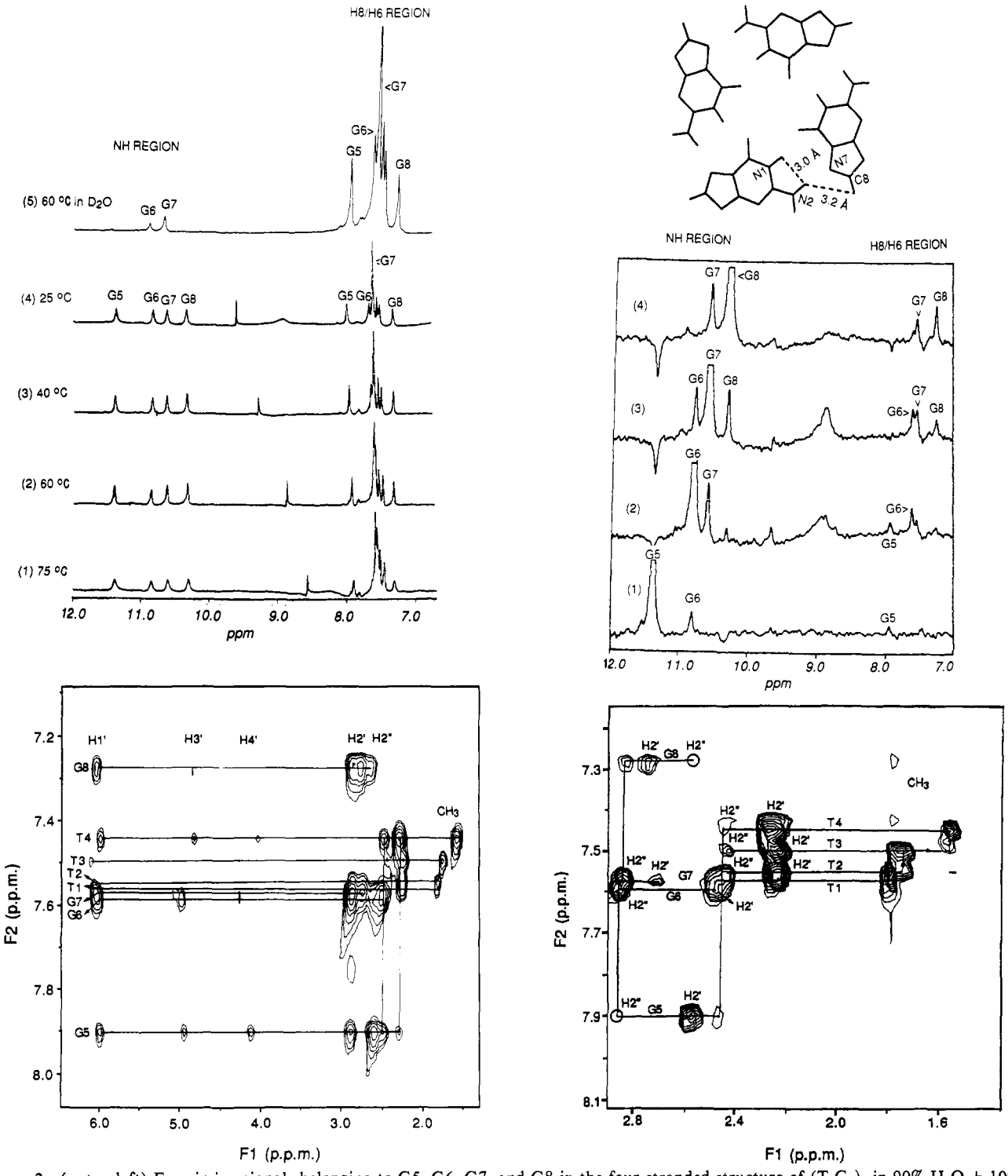

FIGURE 2: (a, top left) Four imino signals belonging to G5, G6, G7, and G8 in the four-stranded structure of $(T_4G_4)_4$ in 90% H_2O + 10% D_2O at different temperatures. Four exchangeable protons in the spectrum occur in the low-field region corresponding to H-bonded G ring protons in dT_4G_4 as opposed to eight in the hairpin, $dG_4T_4G_4$ (Smith & Feigon, 1992). Note that the imino signals remain essentially the same within a range of 25–75 °C and even up to 80 °C (data not shown). Even in 100% D_2O and at 60 °C the imino protons belonging to the two internal bases in the G-tract (i.e., G6 and G7) are still present. Such a behavior is consistent with a well-stacked G-quartet with a H-bonding network as shown in the inset of panel b and Figure 1d. The sharp spike in the middle of the spectra is an artifact. Note the presence of a broad signal near 9 ppm at 25 °C; this signal probably corresponds to the unpaired (exchangeable) NH signals of the thymines. (b, top right) 1D difference NOE spectra of $(T_4G_4)_4$ in 90% H_2O + 10% D_2O in which four imino protons are irradiated (*presaturation time* = 1 s, temperature = 60 °C). Spectra 1–4 correspond to the 1D NOE profiles in which the NH protons of G5, G6, G7, and G8 are respectively irradiated. (Inset) The NOE pathway is indicated, suggesting how H8 of G in a given layer of G-quartet should show NOE when N1-H in the same G-layer is irradiated. Intra- and interlayer NOEs (as discussed in the text) allow sequential assignment of the NH and H8 protons of G5, G6, G7, and G8. The strongest NOE signals in each spectrum correspond to NH(*i*)···NH(*i*+1) interactions; NH(*i*)···H8(*i*) NOEs are weaker than NH(*i*)···NH(*i*+1) NOEs while H8(*i*–1)···NH(*i*) NOEs are weaker than H8(*i*)···NH(*i*) NOEs and H8(*i*+1)···NH(*i*) NOEs are weakest in the spectra. The NOE at H8 in the G5-layer is the weakest among four G-layers (compare spectra 2, 3, and 4 with spectrum 1) probably due to reduced rigidity (or higher mobility) of the G5's in this layer of G-quartet at 60 °C. It is not clear why noticeable negative (nonspecific) NOEs appear at NH(G5) in spectra 3 and 4. (c, bottom left) NOESY (τ_m = 100 ms) cross section showing connectivities between base protons (G H8 and T H6) and sugar protons (H1′-H4′) as well as T H6–T CH_3 and G5 H8–T CH_3 interactions. Extensive overlap of the H5′,H5″ region precluded assignment of these sugar protons. (d, bottom right) ROESY (τ_m = 60 ms) cross section showing interactions of G H8 and T H6 protons with H2′,H2″ sugar protons and T CH_3 protons. The carrier offset was set to the HDO peak frequency, and a spin-lock power of 4 kHz was applied during the mixing phase. All cross-peaks shown correspond to positive NOEs.

1D NOE experiments, as shown in Figure 2b. In addition, the data presented in panels a and b of Figure 2 show that while all G's are associated in four layers of stacked G-tetrads, at 60 °C, the T's do not form stable H-bonded pairs as evidenced by the lack of signals from slowly exchanging T NH protons.

2D NOESY/ROESY Experiments. As explained below, the structure of the dT_4G_4 tetraplex consists of two conformationally distinct domains: a rigid core of the structure containing the G clusters (G5, G6, G7, and G8), the stacked flanking T4 plane, and a flexible tail containing T1, T2, and T3. The local dynamics of these regions are quite different. The nucleotides in the rigid core of the structure have longer effective correlation times, thereby allowing measurement of intra- and internucleotide NOEs along the strand. The nucleotides in the flexible tail, on the contrary, have shorter correlation times, thereby eluding the measurement of key internucleotide NOEs in a laboratory frame NOESY experiment. However, this problem is overcome by performing the rotating frame Overhauser enhancement experiment (ROESY). In the ROESY experiment ROEs are observed for all pairwise interactions below a certain distance limit (usually <4 Å) irrespective of the corresponding correlation time (long or short). Therefore, NOESY and ROESY are both used for sequential assignment and structure determination.

Sequential Assignment. Four G H8 resonances are already assigned in Figure 2b. Figure 2c shows a cross section of the 2D ^1H NOESY spectrum of dT_4G_4 in D_2O. In this cross section four distinct G H8 resonances and four T H6 resonances are detected, confirming that each dT_4G_4 strand in the tetramer has the identical chemical shifts and environment. The cross-peaks on the horizontal lines drawn through the chemical shift values of H8/H6 enable us to identify the spin systems (H8/H6, H1′, H2′, H2″, H3′, H4′) belonging to eight different nucleotides. The H2′ and H2″ resonances for a given residue are distinguished by intraresidue H8/H6···H2′,H2″, H1′···H2′, H2″, and H3′···H2′,H2″ connectivities. We observe stronger intranucleotide NOEs for the H8/H6···H2′, H1′···H2″, and H3′···H2′ proton pairs and weaker NOEs for the H1′···H2′, H8/H6···H2″, and H3′···H2″ proton pairs, as expected for a C2′-*endo*, *anti* nucleotide conformation. The internucleotide connectivities involving H2″(i–1)···H8/H6(i) allow sequence-specific assignment of the spin systems (H8/H6, H2′, H2″) belonging to T4, G5, G6, G7, and G8 in the rigid core of the structure. The remaining protons (i.e., H1′, H3′, H4′) in the spin systems of these five nucleotides are identified by examining H1′,H3′···H2′,H2″ and H3···H4′ NOESY cross sections.

As described above, the T's in the flexible tail of the structure (i.e., T1, T2, T3) do not show internucleotide NOESY cross-peaks because of the lack of a defined conformational preference for the nucleotides T1, T1, and T3. A rotating frame Overhauser enhancement spectroscopy experiment (ROESY) (Bax, 1988) overcomes this, as shown in Figure 2d. Monitoring the sequential H6(i)···CH_3(i+1) internucleotide NOE pattern in the combined NOESY and ROESY experiments allows us to trace the T1 → T2 → T3 → T4 pathway. Because of the partial overlap of H6/CH_3 of T1 and T2, we determined the center of the T1 resonance from the ROESY experiment as that CH_3 group showing a CH_3···CH_3 NOE only to its 3′ neighbor and by comparing NOESY/ROESY slices through the H8/H6 section of T1 and T2 to identify the weaker intranucleotide H6···CH_3 interaction as that of the terminal T1.

Table I shows the chemical shift values of different protons in the dT_4G_4 tetraplex obtained from combining NOESY and ROESY data.

Table I: Chemical Shift Values of Various Protons in the dT_4G_4 Tetramer at 60 °C with Respect to TSP as Internal Standard

	H8/H6	CH_3	H1′	H2′	H2″	H3′	H4′	NH
T1	7.57	1.76	6.03	2.43	2.43	4.93	4.20	nv[a]
T2	7.55	1.76	6.03	2.19	2.42	4.75	4.09	nv
T3	7.50	1.69	6.06	2.18	2.42	4.75	4.09	nv
T4	7.45	1.53	5.96	2.22	2.43	4.75	4.09	nv
G5	7.90		5.98	2.57	2.85	4.90	4.20	11.38
G6	7.60		5.98	2.46	2.84	4.90	4.30	10.81
G7	7.58		5.98	2.67	2.83	5.02	4.30	10.60
G8	7.27		5.99	2.76	2.63	4.78	4.21	10.33

Conformational Details of the dT_4G_4 Tetramer. The presence of strong intranucleotide H8···H2′ NOEs with weak intranucleotide H8···H1′/H3′ NOEs (in Figure 2c) indicates that each G nucleotide in the complex has the C2′-*endo*, *anti* conformation (Gupta et al., 1989). No G's in a *syn* conformation are present; these would give strong intranucleotide H8···H1′ NOEs (Smith & Feigon, 1992), which are not seen. The H8/H6 aromatic resonances are sufficiently distinct in chemical shift to allow identification of each of the intra- and internucleotide NOEs, except for partial overlapping of the H8 of G6 with G7 and the H6 of T1 with T2. Since the H2′, H2″ spin systems of G6 and G7 differ in chemical shift, the NOEs from H8 (G6/G7) are obtained by monitoring appropriate NOESY slices. It should be noted that the overlap of H1′ resonances in this molecule precludes identification of individual sugar pucker by phase-sensitive COSY or DQF-COSY experiments (Wuthrich, 1986).

Four identical strands in a tetramer with all G's *anti* can only form a right-handed helical tetraplex (Sundquist & Klug, 1989) with a parallel strand orientation:

$$^{anti}G\text{–}G^{anti}$$

$$^{anti}G\text{–}G^{anti}$$

By contrast, the hairpin dimer structure formed by $G_4T_4G_4$ consists of alternating *syn–anti* G residues in an antiparallel array (Kang et al., 1992):

$$^{syn}G\text{–}G^{anti}$$

$$^{anti}G\text{–}G^{syn}$$

All G's in the dT_4G_4 tetramer show H8(i+1)···H2″(i) internucleotide NOE connectivities, defining four stacked G layers in the structure. If the G's were in the C3′-*endo*, *anti* conformation, a strong sequential pattern of H8(i+1)···H2′-(i) connectivities should be observed; these are not present on examining H8 slices of the NOESY spectrum. The internucleotide H8(i+1)···H2″(i) NOE connectivity extends to the T4-G5 step, so that T4 must be stacked over the G5-layer in a right-handed helical conformation. All the T's in the structure have the C2′-*endo*, *anti* conformation. However, unlike T4, the T's in the flanking tail (i.e., T1, T2, T3) are flexible, and they sample several stacked and unstacked conformations while still retaining the average C2′-*endo*, *anti* conformation.

FMNS and MD Simulated Annealing: Derivation of a Detailed Structural Model of the Parallel-Stranded dT_4G_4 Tetramer. A structural model for the parallel-stranded tetramer of dT4G4 in solution is derived from the NMR data by means of FMNS and MD simulated annealing as outlined in Materials and Methods. The relaxation matrix contained (78 × 78) elements with contributions from pairwise interactions due to nonexchangeable protons (H8/H6, CH_3, H1′, H2′, H2″, H3′, H4′, H5′, H5″), belonging to four G's and four T's. After a set of stereochemically allowed structures with low *R*-factors were selected (Gupta et al., 1989), a set

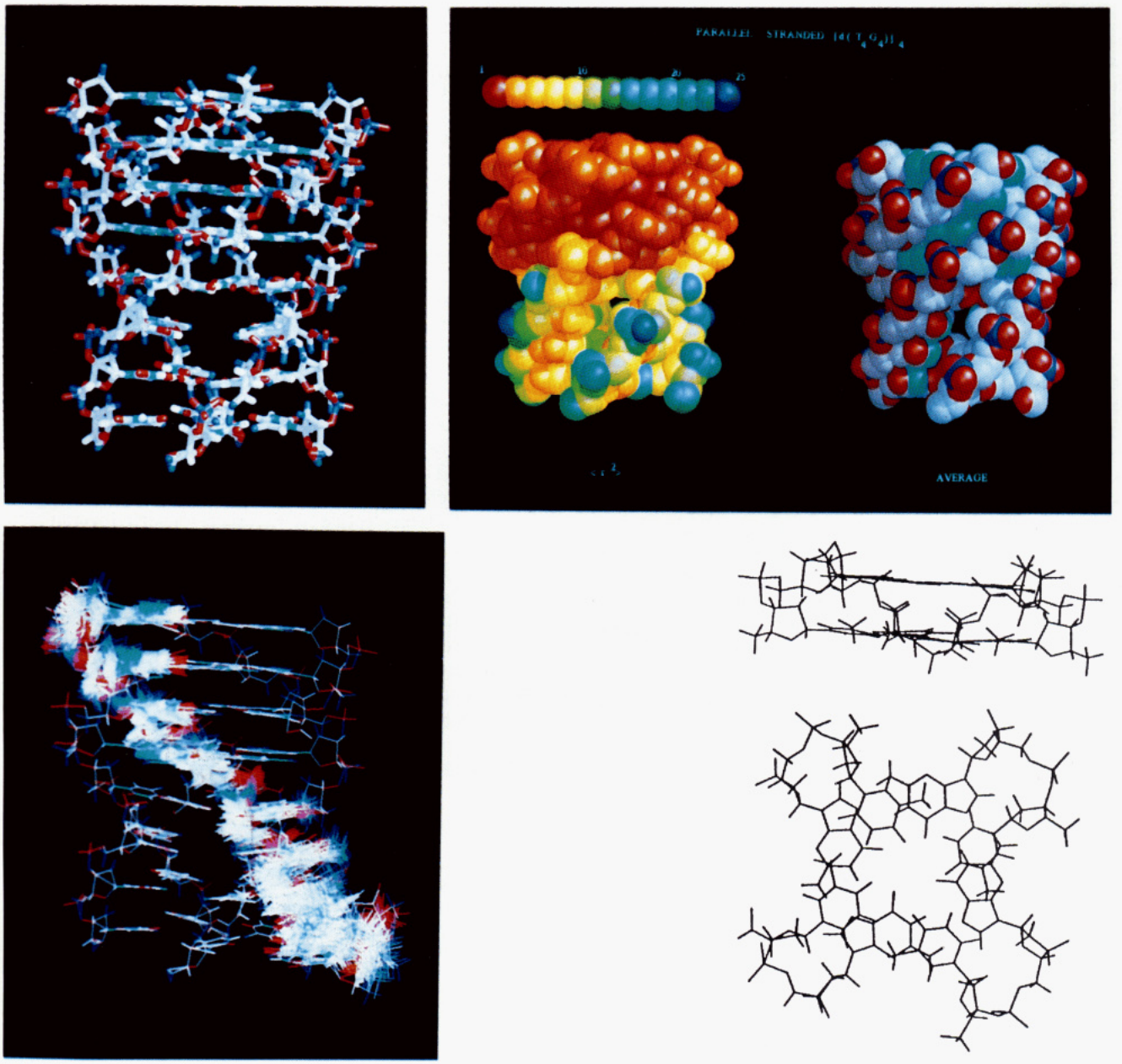

FIGURE 3: Panel a (top left) shows an energy-minimized structure representative of the averaged sampled configurations. Eight planes containing four G's and four T's result, with those in the T planes having much greater rms fluctuations than the G's. Panel b (top right) shows a space-filling representation of the same structure. The molecule is shown on the right with different atoms colored according to atom type (oxygen = red, carbon = white, nitrogen = light blue, and phosphorus = dark blue). The left-hand side shows a representation of the same molecule with the atoms color-coded according to the mean square displacement exhibited by the atom in the 160 sampled conformations. The relation between the color codes and the mean square displacements (in Å^2) is given in the colored bar shown on top of the figure. The average rms for different base planes is rms(T1) = 3.3 Å > rms(T2) = 2.8 Å > rms(T3) = 2.7 Å > rms(T4) = 2.3 Å. The four G layers show rms fluctuations of around 1.0 Å or less. Panel c (bottom left) shows a superposition of 40 sampled structures of one T4G4 strand. This illustrates the large variation exhibited by the T's relative to the variations in the G's. Panel d (bottom right) shows side and top views of the stacking at the T4-G5 step. Each T stacks partially below two G bases in the G5 layer, in an interaction that appears to be stabilized by a K^+ ion located between the planes. While repulsion between the methyl groups and O2 (3.1 Å apart) seems to exclude H-bonding between N3 and O4 (3.5 Å apart), these two atoms have a favorable electrostatic interaction. In the absence of a localized K^+ ion, the four T's can associate in a different mode, with the four methyls clustering in the center of the plane and O2 and O4 both exposed to solvent.

of interproton distances were extracted as independent structural constraints that are required for agreement with NOESY/ROESY data. These structural constraints included the following distance ranges: (i) intranucleotide distances for each nucleotide, H8/H6···H2′ (2.1–2.8 Å), H8/H6···H2″ (3.4–4.2 Å), H8/H6···H1′ (3.6–4.1 Å), and H8/H6···H3′ (3.8–4.5 Å); (ii) internucleotide distances inside the G-tract, H2″-(*i*–1)···H8(*i*) (2.1–2.5 Å), H2′(*i*–1)···H8(*i*) (3.5 ± 0.5 Å), and H8(*i*–1)···H8(*i*) (3.3–4.3 Å); (iii) similar internucleotide distances in the T4–G5 step and internucleotide distances inside the G-tract, H2″(T4)···H8(G5) (2.1–2.7 Å) and H1′-(T4)···H8(G5) (3.3–4.3 Å); (iv) upper bounds for the T H6-(*i*)···CH_3(*i*+1)/H2″(*i*)···H6(*i*+1) distances in the flexible T-tract (this set of distances, usually 4 Å, was provided by the ROESY data); (v) H-bonding distances as evident from Figure 2a,b (four distances correspond to each G in the quartet as shown in the inset of Figure 2b).

A total of 180 independent distance constraints were included in the calculations (45 interproton distances for each strand). The Cartesian coordinates and tables of expected and actual distances in the models can be obtained from the authors on request. Distance constraints are consistent with a right-handed helical structure of dT_4G_4 with all nucleotides in the C2′-*endo*, *anti* conformation. The 100-ps MD simu-

lation and subsequent energy minimization of the MD snapshots at 1-ps intervals resulted in 100 energy-minimized structures, consistent with the NMR data presented in Figure 2a–d. Four K^+ ions were explicitly included in the MD and energy-minimization calculations. The model of the parallel-stranded dT_4G_4 tetramer in Figure 3a corresponds to the ensemble average of the 100 sampled local minima, each satisfying the distance constraints derived from the NMR data. Even though in the average structure eight planes containing 4G's or 4T's appear to show well-defined stacked layers, only the four G-layers show small rms fluctuations (1.0 Å or less) while, as shown in Figure 3b, the T planes have large rms deviations around the average positions [rms(T1) = 3.3 Å > rms(T2) = 2.8 Å > rms(T3) = 2.7 Å > rms(T4) = 2.3 Å]. The $\langle r^2 \rangle$ deviations of all the atoms with respect to the average positions are also shown in Figure 3b. The phosphate groups connecting two T's in the T-tail have the largest deviations from the average values. This explains the effective short correlation time for the internucleotide distances in the T-tract and, therefore, the absence of the corresponding cross-peaks in the conventional laboratory frame NOESY experiment. Among the four T's, T4 is the least flexible. The lower flexibility of the T4-layer can be seen in Figure 3c, which is a superposition of the individual structures of 40 members of the set of annealed conformations. As seen in Figure 3d, each T in the T4-layer is partially stacked across two G's in the G5-layer. This stacking is possibly stabilized by a K^+ ion located between the T4- and G5-planes.

DISCUSSION

The NMR data described above reveal the following structural features of the parallel-stranded dT_4G_4 tetramer. (1) A single copy of the *Oxytricha* telomeric DNA sequence dT_4G_4 forms an exceptionally stable parallel-stranded tetramer in which four layers of G-quartets are ordered in a helical array while, aside from T4, the T's do not form a detectable H-bonded network and sample multiple stacked configurations. (2) T4, adjacent to the G-layer, shows a right-handed helical structure similar to that of the G-tract. (3) While a rigid G4-tract and more flexible T-tract coexist in the same structure, the overall structure is extremely stable. The ring protons of the G core exchange very slowly, implying exceptional stability within this structure. Exchange from the surface layers (G5 and G8) is probably mediated by direct solvent contact with water, since the interior of the structure (G6 and G7) requires days to exchange even at 60 °C. The behavior of the T's is different. The T4-layer clearly interacts with G5, possibly via metal H-bonding to this layer, while the remaining T's sample an extended conformational space in which electrostatic effects are probably important, since shorter T-tracts are more stable than longer ones (Lu et al., unpublished data). While repulsion between the methyl groups of T4 and O2 of G5 (3.1 Å apart) would seem to exclude H-bonding between N3 and O4 (3.5 Å apart), these two atoms show a favorable electrostatic interaction. A bound K^+ might favor this interaction. In the absence of a localized ion the four T's are seen to associate in a different mode in the simulations, with the four methyls clustered in the middle of the layer and O2 and O4 exposed to the solvent. It may be noted that tetraplex structures involving putative G-quartets as shown in Figure 1d have been reported in the literature on G-monomers (Gellert et al., 1962). However, models based on fiber diffraction data (Sasisekharan et al., 1975) do not provide direct information about the nucleotide conformation in these structures. The X-ray model of Kang et al. (1992) provides a detailed picture of the geometry of a quartet, but with a quite different pattern of folding of the backbone, with alternating *syn* and *anti* G nucleotides.

The fact that unitary dT_4G_4 strands associate to form this parallel-stranded tetraplex suggests that this is the most stable state for chains with one copy of telomeric sequences. This is consistent with the exceptional thermal stability of the structure, which is only partially unfolded at 100 °C in the presence of 200 mM K^+ (Lu et al., 1992). In addition, direct comparison of the thermal stability of the parallel *vs* antiparallel structures in the same background reveals significantly higher stability for the parallel structure (Lu et al., 1993). Why then do repeats of this sequence fail to assume this state? Kinetically, we find that parallel tetraplex formation in tandem repeats of telomeric sequences is slow *in vitro*, because of the relative ease of hairpin formation but not because of any intrinsic conformational barrier (Lu et al., 1993). The parallel form is strongly responsive to K^+ also, relative to hairpin structures. The conclusion that telomeric sequences can assume inherently different structures, depending on the nature of the processes that lead, for example, to ablation of telomeric sequences or damage at the ends of a chromosome, seems important in trying to understand the biology of chromosomes. Factors such as the local concentration of free ends or strands, as well as the sodium–potassium ratio (Sen & Gilbert, 1988), can regulate the conformation of the G clusters, which acting alone or together can lead to cohesion of these regions following damage.

REFERENCES

Acevedo, O. L., Dickinson, L. A., Macke, T. J., & Thomas, C. A., Jr. (1991) *Nucleic Acids Res. 19*, 3409–3419.

Arnott, S., Chandrasekaran, R., & Marttila, C. M. (1974) *Biochem. J. 141*, 537–543.

Bax, A. (1988) *J. Magn. Reson. 77*, 134–147.

Blackburn, E. (1991) *Nature 350*, 569–571.

Gellert, M., Lipsett, M. N., & Davies, D. R. (1962) *Proc. Natl. Acad. Sci. U.S.A. 48*, 2013–2018.

Gupta, G., Umemoto, K., Sarma, M. H., & Sarma, R. H. (1989) *Int. J. Quantum Chem., Quantum Biol. Symp. 16*, 17–33.

Gupta, G., Garcia, A. E., & Hiriyanna, K. T. (1993) *Biochemistry 32*, 948–960.

Henderson, E. R., & Blackburn, E. H. (1989) *Mol. Cell. Biol. 9*, 345–348.

Henderson, E. R., Hardin, C. C., Walk, S. K., Tinoco, I., & Blackburn, E. H. (1987) *Cell 51*, 899–908.

Hope, I. A., & Struhl, K. (1987) *EMBO J. 6*, 2781–2784.

Kang, C., Zhang, X., Ratliff, R., Moyzis, R., & Rich, A. (1992) *Nature 356*, 126–131.

Klobutcher, L. A., Swanton, M. T., Donini, P., & Prescott, D. M. (1981) *Proc. Natl. Acad. Sci. U.S.A. 78*, 3015–3019.

Lu, M., Guo, Q., & Kallenbach, N. R. (1992) *Biochemistry 31*, 2455–2459.

Lu, M., Guo, Q., & Kallenbach, N. R. (1993) *Biochemistry 32*, 589–601.

Sen, D., & Gilbert, W. (1988) *Nature 334*, 364–366.

Sen, D., & Gilbert, W. (1990) *Nature 344*, 410–414.

Sen, D., & Gilbert, W. (1992) *Biochemistry 31*, 65–70.

Smith, F. W., & Feigon, J. (1992) *Nature 356*, 164–168.

Stillinger, F. H., & Weber, T. A. (1984) *Science 225*, 983–993.

Sundquist, W. I., & Klug, A. (1989) *Nature 342*, 825–829.

Williamson, J. R., Raghuraman, M. K., & Cech, T. R. (1990) *Cell 59*, 871–880.

Wuthrich, K. (1986) *NMR of Proteins and Nucleic Acids*, pp 203–251, Wiley, New York.

Yu, G.-L., & Blackburn, E. H. (1991) *Cell 67*, 823–832.

Zimmerman, S. B., Cohen, G. H., & Davies, D. R. (1975) *J. Mol. Biol. 92*, 181–192.